

# Boundary Layer Transient Hygroscopic Stresses in Orthotropic Thick Shells Under External Pressure

G. A. Kardomateas  
Associate Professor.

C. B. Chung  
Graduate Research Assistant.

School of Aerospace Engineering,  
Georgia Institute of Technology,  
Atlanta, GA 30332-0150

*An exact elasticity solution is obtained for the stresses and displacements in an orthotropic cylindrical shell loaded by an external pressure under imposed constant moisture concentrations on the inner and outer surfaces. The material properties are assumed moisture independent and a displacement approach is used. Since the moisture diffusion process is relatively slow, the hygroscopic stresses are confined for practical time values to a boundary layer region near the surfaces. Illustrative results are presented for graphite-epoxy material regarding the boundary layer hygroscopic effect on the stress field with respect to time and the coupling of mechanical loading (external pressure) and moisture diffusion. For this material, it is shown that this effect is more pronounced for the axial component of stress.*

## Introduction

The understanding of the stresses induced by moisture in a composite structure is essential for the design and the comprehensive study of its response during service in severe hygroscopic environments. It is well known that a polymeric resin absorbs moisture from its environment. Whitney and Husman (1978) showed that the absorption of moisture from severely hygroscopic environments reduces the modulus and the strength of a resin-based composite. Wang and Choi (1982) suggested that an unanticipated failure of a composite structure, frequently initiated at the edges, can be a result of hygroscopic stresses near the edges.

The hygroscopic stress field in the vicinity of laminate plate boundaries, i.e., the so-called hygroscopic boundary layer stresses, which might be primarily responsible for strength degradation and failure of composites, has been investigated by several researchers using different approximate methods (e.g., Farley and Herakovich, 1978; Crossman and Wang, 1978). The high hygroscopic stresses are also reported to be confined within a localized region of several lamina thicknesses from the edge, and in the boundary layer region they cannot be assessed accurately with classical lamination theory.

The behavior of this highly stressed boundary layer region is of great importance in controlling the complex failure modes

and performance of the composite. Accurate quantitative assessment of the hygroscopic boundary layer stresses is essential to the design, failure analysis, and serviceability of composite structures.

Although the majority of hygroelastic analyses have been performed in plate structures, some studies have also been reported in thin shell geometries. In particular, Lee and Yen (1988) showed that the moisture absorption can degrade the buckling load in a composite shell structure subjected to compression. Doxee and Springer (1989) analyzed hygrothermal stresses and strains in an axisymmetric composite shell according to their higher order shell theory.

In view of the fairly thick construction envisioned for composite shells in marine applications, there is a need to investigate the stress and strain fields induced by the joint action of moisture absorption and mechanical (pressure) loading in a thick composite shell structure. To this extent, an elasticity solution would provide accurate results for certain simple configurations, but, more importantly, would form a basis for comparing various shell theories that could be potentially used for more complex geometries.

In this work, the problem of transient hygroscopic stresses in a hollow orthotropic circular cylinder loaded by external pressure is examined. It is assumed that both the inner and outer surfaces are at constant (but different) concentrations of moisture. The material properties are assumed independent of the concentration of moisture. It is also assumed that there is only radial dependence of the moisture concentration field. In a related study, Kardomateas (1989, 1990) used a displacement approach and a series expansion technique to solve the transient thermal stress problem in composite cylinders. In this paper, the displacement approach will be used to analyze the coupled transient moisture diffusion and mechanical loading

Contributed by the Applied Mechanics Division of THE AMERICAN SOCIETY OF MECHANICAL ENGINEERS for publication in the ASME JOURNAL OF APPLIED MECHANICS.

Discussion on this paper should be addressed to the Technical Editor, Professor Lewis T. Wheeler, Department of Mechanical Engineering, University of Houston, Houston, TX 77204-4792, and will be accepted until four months after final publication of the paper itself in the ASME JOURNAL OF APPLIED MECHANICS.

Manuscript received by the ASME Applied Mechanics Division, June 23, 1992; final revision, Feb. 4, 1993. Associate Technical Editor: R. M. Bowen.

(external pressure) problem. Numerical results are presented for the stresses with respect to time and the radial coordinates for an example case of graphite/epoxy material. The results illustrate clearly the nature of the transient hygroscopic boundary stress layer.

### Mathematical Formulation

Consider a hollow cylinder, in general under external pressure  $p$ , as shown in Fig. 1. The cylinder has an inner radius,  $r_1$  and an outer radius,  $r_2$ . The radial, circumferential, and axial coordinates are denoted by  $r$ ,  $\theta$ , and  $z$ , respectively. It is assumed that the initial concentration (at  $t = 0$ ) is  $C_0$ . For  $t > 0$ , the boundaries  $r = r_1$  and  $r = r_2$  are kept at constant concentrations  $C_1$  and  $C_2$ , respectively. The reference concentration is taken as zero. The moisture problem is solved by the Fickian diffusion equation

$$\frac{\partial C(r, t)}{\partial t} = D \frac{1}{r} \frac{\partial}{\partial r} \left( r \frac{\partial C}{\partial r} \right) \quad r_1 \leq r \leq r_2, \quad (1a)$$

where  $C(r, t)$  is the moisture concentration and  $D$  is the moisture diffusivity of the composite in the  $r$  direction. The initial and boundary conditions are

$$C(r, t=0) = C_0 \quad r_1 \leq r \leq r_2, \quad (1b)$$

$$C(r_1, t) = C_1 \quad \text{and} \quad C(r_2, t) = C_2 \quad t > 0, \quad (1c)$$

where  $C_0$ ,  $C_1$ , and  $C_2$  are constants. Crank (1975) gives the general solution for the distribution of the concentration of moisture  $C(r, t)$  to Eq. (1) in terms of the Bessel functions of the first and second kind  $J_n$  and  $Y_n$ , as follows:

$$C(r, t) = b_1 \ln(r/r_1) + b_2 \ln(r_2/r) + \sum_{n=1}^{\infty} [c_n J_0(r\alpha_n) + d_n Y_0(r\alpha_n)] e^{-D\alpha_n^2 t}, \quad (2a)$$

where

$$b_1 = \frac{C_2}{\ln(r_2/r_1)}; \quad b_2 = \frac{C_1}{\ln(r_2/r_1)}, \quad (2b)$$

$$c_n = \pi C_0 \frac{J_0(r_1\alpha_n) Y_0(r_2\alpha_n)}{J_0(r_1\alpha_n) + J_0(r_2\alpha_n)} - \pi J_0(r_1\alpha_n) Y_0(r_2\alpha_n) \frac{C_2 J_0(r_1\alpha_n) - C_1 J_0(r_2\alpha_n)}{J_0^2(r_1\alpha_n) - J_0^2(r_2\alpha_n)}, \quad (2c)$$

$$d_n = -\pi C_0 \frac{J_0(r_1\alpha_n) J_0(r_2\alpha_n)}{J_0(r_1\alpha_n) + J_0(r_2\alpha_n)} + \pi J_0(r_1\alpha_n) J_0(r_2\alpha_n) \frac{C_2 J_0(r_1\alpha_n) - C_1 J_0(r_2\alpha_n)}{J_0^2(r_1\alpha_n) - J_0^2(r_2\alpha_n)}, \quad (2d)$$

and  $\alpha_n$  are the positive roots of

$$J_0(r_1\alpha_n) Y_0(r_2\alpha_n) - J_0(r_2\alpha_n) Y_0(r_1\alpha_n) = 0. \quad (2e)$$

The hygroscopic stress-strain relations for the orthotropic body are

$$\begin{bmatrix} \sigma_{rr} \\ \sigma_{\theta\theta} \\ \sigma_{zz} \\ \tau_{\theta z} \\ \tau_{rz} \\ \tau_{r\theta} \end{bmatrix} = \begin{bmatrix} c_{11} & c_{12} & c_{13} & 0 & 0 & 0 \\ c_{12} & c_{22} & c_{23} & 0 & 0 & 0 \\ c_{13} & c_{23} & c_{33} & 0 & 0 & 0 \\ 0 & 0 & 0 & c_{44} & 0 & 0 \\ 0 & 0 & 0 & 0 & c_{55} & 0 \\ 0 & 0 & 0 & 0 & 0 & c_{66} \end{bmatrix} \begin{bmatrix} \epsilon_{rr} - \beta_r \Delta C \\ \epsilon_{\theta\theta} - \beta_\theta \Delta C \\ \epsilon_{zz} - \beta_z \Delta C \\ \gamma_{\theta z} \\ \gamma_{rz} \\ \gamma_{r\theta} \end{bmatrix}, \quad (3)$$

where  $c_{ij}$  are the elastic constants and  $\beta_i$  the swelling coefficients (1, 2, and 3 represent  $r$ ,  $\theta$ , and  $z$ , respectively). The geometry (Fig. 1) is axisymmetric. Since the moisture concentration is assumed to depend only on the  $r$  direction, the stresses are independent of  $\theta$  and  $z$  and the hoop displacement is zero. In

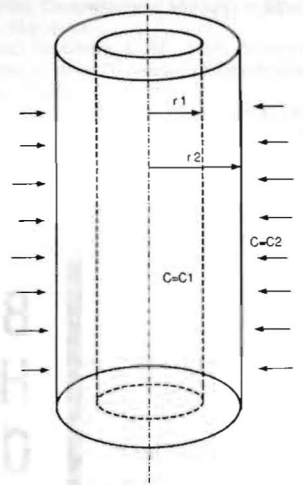


Fig. 1 Thick cylindrical shell under constant boundary concentrations of moisture

addition to the constitutive Eq. (3), the equilibrium equations have to be satisfied; since  $\tau_{r\theta} = \tau_{rz} = \tau_{\theta z} = 0$ , only one equilibrium equation remains:

$$\frac{\partial \sigma_{rr}}{\partial r} + \frac{\sigma_{rr} - \sigma_{\theta\theta}}{r} = 0. \quad (4)$$

In this work the displacement field derived by Lekhnitskii (1981) for time-independent problems and modified by Kardomateas (1989) for time-dependent thermal stress problems (which are analogous to the time-dependent moisture-induced stress problems) is used:

$$\begin{aligned} u_r &= U(r, t) + z(w_y \cos \theta - w_x \sin \theta) + u_0 \cos \theta + v_0 \sin \theta, \\ u_\theta &= -z(w_y \sin \theta + w_x \cos \theta) + w_z r - u_0 \sin \theta + v_0 \cos \theta, \\ u_z &= z f(t) - r(w_y \cos \theta - w_x \sin \theta) + w_0, \end{aligned} \quad (5)$$

where the function  $U(r, t)$  represents the radial displacement accompanied by deformation. The constants  $u_0$ ,  $v_0$ , and  $w_0$  denote the rigid-body translation along the  $x$ ,  $y$ , and  $z$  directions in the Cartesian coordinate system, respectively, and  $w_x$ ,  $w_y$ , and  $w_z$  denote the rigid-body rotation in the  $x$ ,  $y$ , and  $z$  directions (these may also be functions of time, but since they do not appear in the strain expressions, such a dependence would not affect the expressions that follow in this section).

The parameter  $f(t)$  is obtained from boundary conditions, as discussed later. The strains are expressed in terms of the displacements as follows:

$$\begin{aligned} \epsilon_{rr} &= \frac{\partial U(r, t)}{\partial r}, \quad \epsilon_{\theta\theta} = \frac{U(r, t)}{r}, \quad \epsilon_{zz} = f(t), \\ \gamma_{\theta z} &= \gamma_{zr} = \gamma_{r\theta} = 0. \end{aligned} \quad (6)$$

Substituting Eqs. (6) and (3) into the equilibrium Eq. (4) gives the following differential equation for  $U(r, t)$ :

$$\begin{aligned} c_{11} \left[ \frac{\partial^2 U(r, t)}{\partial r^2} + \frac{1}{r} \frac{\partial U(r, t)}{\partial r} \right] - \frac{c_{22}}{r^2} U(r, t) \\ = q_1 \frac{\partial C(r, t)}{\partial r} + q_2 \frac{C(r, t)}{r} + (c_{23} - c_{13}) \frac{f(t)}{r}, \end{aligned} \quad (7a)$$

where

$$q_1 = c_{11} \beta_r + c_{12} \beta_\theta + c_{13} \beta_z, \quad (7b)$$

$$q_2 = (c_{11} - c_{12}) \beta_r + (c_{12} - c_{22}) \beta_\theta + (c_{13} - c_{23}) \beta_z. \quad (7c)$$

Now set  $f(t)$  in the form

$$f(t) = f_0 + \sum_{n=1}^{\infty} f_n e^{-D\alpha_n^2 t}. \quad (8)$$

Moreover, to solve Eq. (7), set

$$U(r, t) = U_0(r) + \sum_{n=1}^{\infty} R_n(r) e^{-D\alpha_n^2 t} \quad (9)$$

Substituting Eqs. (2), (8), and (9) into Eq. (7a) yields the following equations to be satisfied for  $U_0$ , and  $R_n$  for  $n = 1, 2, \dots, \infty$ :

$$c_{11}U_0''(r) + \frac{c_{11}}{r}U_0'(r) - \frac{c_{22}}{r^2}U_0(r) = \frac{c_{23} - c_{13}}{r}f_0 + q_1 \frac{b_1 - b_2}{r} + q_2 b_1 \frac{\ln(r/r_1)}{r} + q_2 b_2 \frac{\ln(r_2/r)}{r}, \quad (10a)$$

$$c_{11}R_n''(r) + \frac{c_{11}}{r}R_n'(r) - \frac{c_{22}}{r^2}R_n(r) = \frac{c_{23} - c_{13}}{r}f_n + c_n \left[ q_2 \frac{J_0(r\alpha_n)}{r} - q_1 \alpha_n J_1(r\alpha_n) \right] + d_n \left[ q_2 \frac{Y_0(r\alpha_n)}{r} - q_1 \alpha_n Y_1(r\alpha_n) \right] \quad n = 1, \dots, \infty. \quad (10b)$$

For each of the previous equations, the solution is the sum of a homogeneous solution and a particular one. The solution of the homogeneous equation is in the form  $G_1(t)r^{\lambda_1} + G_2(t)r^{\lambda_2}$  with

$$\lambda_{1,2} = \pm \sqrt{c_{22}/c_{11}}. \quad (10c)$$

In a similar fashion to the parameter  $f(t)$ , set  $G_i(t)$  in the form:  $G_i(t) = G_{i0} + \sum G_{in} e^{-D\alpha_n^2 t}$ ,  $i = 1, 2$ .

Since the constants  $f_n$  and  $G_{ij}$  are yet unknown, we shall indicate the places where they enter in the expressions that follow (these constants are found later from the boundary conditions). For  $c_{11} \neq c_{22}$ , the solution of (10a) for  $U_0(r)$  is

$$U_0(r) = G_{10}r^{\lambda_1} + G_{20}r^{\lambda_2} + \frac{c_{23} - c_{13}}{c_{11} - c_{22}} f_0 r + U_0^*(r), \quad (11a)$$

where

$$U_0^*(r) = \frac{q_2 b_1}{c_{11} - c_{22}} r \ln(r/r_1) + \frac{q_2 b_2}{c_{11} - c_{22}} r \ln(r_2/r) + \frac{[q_1(c_{11} - c_{22}) - 2q_2 c_{11}]}{(c_{11} - c_{22})^2} (b_1 - b_2)r. \quad (11b)$$

For  $c_{11} = c_{22}$ , the corresponding solution of (10a) is

$$U_0(r) = G_{10}r + \frac{G_{20}}{r} + \frac{c_{23} - c_{13}}{2c_{11}} f_0 r \ln(r/r_1) + U_0^*(r), \quad (12a)$$

where

$$U_0^*(r) = \frac{q_2 b_1}{4c_{11}} r \ln^2(r/r_1) - \frac{q_2 b_2}{4c_{11}} r \ln^2(r_2/r) + \frac{(2q_1 - q_2)(b_1 - b_2)}{4c_{11}} r \ln(r/r_1). \quad (12b)$$

To solve (10b) we use the series expansions of the Bessel functions to obtain a series expansion of the right-hand side, as given in Appendix A. In the following,  $\gamma$  stands for the Euler's constant ( $\approx 0.577215 \dots$ ).

For  $c_{11} \neq c_{22}$ , the resulting Eq. (A3) in Appendix A leads to the solution of (10b) for  $R_n$ ,  $n = 1, \dots, \infty$ , as follows:

$$R_n(r) = G_{1n}r^{\lambda_1} + G_{2n}r^{\lambda_2} + \frac{c_{23} - c_{13}}{c_{11} - c_{22}} f_n r + R_n^*(r), \quad (13a)$$

$$R_n^*(r) = B_{0n}r + \frac{2q_2 d_n}{\pi(c_{11} - c_{22})} r \ln(r\alpha_n/2) + \sum_{k=0}^{\infty} B_{1nk} r^{2k+3} \ln(r\alpha_n/2) + B_{2nk} r^{2k+3}, \quad (13b)$$

where

$$B_{0n} = \frac{c_n q_2 + d_n (2/\pi)(q_1 + \gamma q_2)}{c_{11} - c_{22}} - \frac{4c_{11} q_2 d_n}{\pi(c_{11} - c_{22})^2}. \quad (13c)$$

The coefficients in the sum over  $k$  are given in terms of

$$f_{kn} = \left[ c_n - \frac{2d_n}{\pi} \left( 1 + \frac{1}{2} + \dots + \frac{1}{k+1} - \gamma \right) \right] \times [q_2 + 2q_1(k+1)] + \frac{2d_n q_1}{\pi}, \quad (13d)$$

as follows:

$$B_{1nk} = \frac{2d_n (-1)^{k+1} \alpha_n^{2k+2} [q_2 + 2q_1(k+1)]}{\pi 2^{2k+2} [(k+1)!]^2 [c_{11}(2k+3)^2 - c_{22}]}, \quad (14a)$$

$$B_{2nk} [c_{11}(2k+3)^2 - c_{22}] = \frac{(-1)^{k+1} \alpha_n^{2k+2}}{2^{2k+2} [(k+1)!]^2} f_{kn} - B_{1nk} 2c_{11}(2k+3). \quad (14b)$$

In the (unlikely) event that for a certain  $k$ ,  $c_{11}(2k+3)^2 = c_{22}$ , the term in the sum for this  $k$  is replaced by the one in Appendix B.

For  $c_{11} = c_{22}$  the solution of (10b) for  $R_n$  is

$$R_n(r) = G_{1n}r + \frac{G_{2n}}{r} + \frac{c_{23} - c_{13}}{2c_{11}} f_n r \ln(r/r_1) + R_n^*(r), \quad (15a)$$

$$R_n^*(r) = B_{0n}r \ln(r\alpha_n/2) + \frac{d_n q_2}{2\pi c_{11}} r \ln^2(r\alpha_n/2) + \sum_{k=0}^{\infty} B_{1nk} r^{2k+3} \ln(r\alpha_n/2) + B_{2nk} r^{2k+3}, \quad (15b)$$

where

$$B_{0n} = \frac{\pi c_n q_2 + d_n (2q_1 + 2\gamma q_2 - q_2)}{2\pi c_{11}}. \quad (15c)$$

The series expansion for the Bessel functions cannot be used for large arguments; hence, the requirement of including an increasing number of terms and therefore large arguments necessitates finding a particular solution for the "large arguments" domain. This is achieved by using the Hankel asymptotic expansions of the Bessel functions of the first and second kind (see Appendix A). Employing the substitution

$$\rho = r\alpha_n; \quad R_n^{**}(\rho) = R_n^*(r), \quad (16)$$

gives the following equation for  $R_n^{**}(\rho)$

$$c_{11} \alpha_n^2 \left( R_n^{**}(\rho) + \frac{R_n^{**}(\rho)}{\rho} \right) - c_{22} \alpha_n^2 \frac{R_n^{**}(\rho)}{\rho^2} = \sum_{k=0}^{\infty} \frac{(-1)^k \alpha_n \psi_1(k)}{(2k)!(8\rho)^{2k} \rho \sqrt{\pi \rho}} \times \{ (c_n + d_n) (q_2 \sin \rho - a_{1,k} \rho \cos \rho + a_{2,k} \rho^2 \sin \rho) + (c_n - d_n) (q_2 \cos \rho + a_{1,k} \rho \sin \rho + a_{2,k} \rho^2 \cos \rho) \}, \quad (17)$$

where

$$a_{1,k} = q_1 \frac{4k+1}{4k-1} - q_2 \frac{16k}{(4k-1)^2}; \quad a_{2,k} = \frac{16k q_1}{(4k-1)(4k-3)}. \quad (18)$$

and  $\psi_1(k)$  is defined in Appendix A.

The solution of the above equation for the function  $R_n^{**}(\rho)$  is found to be

$$R_n^{**}(\rho) = \sum_{k=0}^{\infty} p_{k,1}^n \rho^{-2k-1/2} \cos \rho + s_{k,1}^n \rho^{-2k-1/2} \sin \rho + p_{k,2}^n \rho^{-2k-3/2} \cos \rho + s_{k,2}^n \rho^{-2k-3/2} \sin \rho. \quad (19a)$$

The coefficients  $p_{k,1}^n, s_{k,1}^n, p_{k,2}^n, s_{k,2}^n$  are determined by considering the terms in the sum that contribute to the terms  $\rho^{-2k-1/2} \cos \rho, \rho^{-2k-1/2} \sin \rho, \rho^{-2k-3/2} \cos \rho, \rho^{-2k-3/2} \sin \rho$  in the right-hand side of (17). Define

$$D_k = \frac{(-1)^k \psi_1(k)}{(2k)! 8^{2k} \alpha_n \sqrt{\pi}} \quad (19b)$$

We obtain the following recursive formulas for  $p_{k,1}^n, s_{k,1}^n$ :

$$p_{k,1}^n c_{11} = p_{k-1,1}^n [c_{11} (2k - 3/2)^2 - c_{22}] - s_{k-1,2}^n c_{11} (4k - 2) + D_k a_{1,k} (c_n + d_n), \quad (20a)$$

$$s_{k,1}^n c_{11} = s_{k-1,1}^n [c_{11} (2k - 3/2)^2 - c_{22}] + p_{k-1,2}^n c_{11} (4k - 2) - D_k a_{1,k} (c_n - d_n), \quad (20b)$$

and for  $p_{k,2}^n, s_{k,2}^n$ :

$$p_{k,2}^n c_{11} = p_{k-1,2}^n [c_{11} (2k - 1/2)^2 - c_{22}] - s_{k-1,1}^n c_{11} 4k - (D_k q_2 + D_{k+1} a_{2,k+1}) (c_n - d_n), \quad (20c)$$

$$s_{k,2}^n c_{11} = s_{k-1,2}^n [c_{11} (2k - 1/2)^2 - c_{22}] + p_{k-1,1}^n c_{11} 4k - (D_k q_2 + D_{k+1} a_{2,k+1}) (c_n + d_n). \quad (20d)$$

The process starts from  $k = 1$  and the starting values for  $k = 0$  are from (17) and (18) as follows:

$$p_{0,1}^n = -\frac{q_1 (c_n + d_n)}{c_{11} \alpha_n \sqrt{\pi}}; \quad s_{0,1}^n = \frac{q_1 (c_n - d_n)}{c_{11} \alpha_n \sqrt{\pi}}, \quad (21a)$$

$$p_{0,2}^n = (-8q_2 + 3q_1) \frac{(c_n - d_n)}{8c_{11} \alpha_n \sqrt{\pi}};$$

$$s_{0,2}^n = (-8q_2 + 3q_1) \frac{(c_n + d_n)}{8c_{11} \alpha_n \sqrt{\pi}}. \quad (21b)$$

An important issue regarding this analysis will be discussed now. The solution (19) is a particular solution of Eq. (17) derived by considering the Hankel asymptotic expansions of the Bessel functions for values of the argument  $\rho = r\alpha_n \geq \rho_{tr} = 18.0$  (see Appendix A), whereas the solution (13b), which will be denoted by  $R_{nS}^*(r)$ , had been derived based on a series expansion for the Bessel functions, for values of the argument  $\rho \leq \rho_{tr}$ . Since for a given root  $\alpha_n$  the argument  $\rho$  ranges from  $r_1\alpha_n$  to  $r_2\alpha_n$ , there may be a transition point from one solution to the other for  $R_n^*(r)$  in the expression (15a). Both solutions are particular ones and may be different. Therefore, at that transition point a homogeneous solution term should be added to (19) so that

$$R_{nL}^{**}(\rho_{tr}) = R_{nS}^*(\rho_{tr}/\alpha_n); \quad R_{nL}^{***}(\rho_{tr})\alpha_n = R_{nS}^{*'}(\rho_{tr}/\alpha_n). \quad (22b)$$

where  $h_{1n}$  and  $h_{2n}$  are determined from the condition of equal value and slope at the transition point

$$R_{nL}^{**}(\rho_{tr}) = R_{nS}^*(\rho_{tr}/\alpha_n); \quad R_{nL}^{***}(\rho_{tr})\alpha_n = R_{nS}^{*'}(\rho_{tr}/\alpha_n). \quad (22b)$$

Thus, the expression for  $U(r, t)$  satisfying the equilibrium equations is obtained with the unknown coefficients  $G_{10}, G_{20}, f_0, G_{1n}, G_{2n}$  and  $f_n$  for  $n = 1, 2, \dots$ . These coefficients are determined from the following boundary conditions:

$$\begin{aligned} \sigma_{rr}(r_1, t) &= 0, \quad \sigma_{rr}(r_2, t) = -p; \\ \tau_{r\theta}(r_i, t) &= \tau_{rz}(r_i, t) = 0, \quad i = 1, 2 \end{aligned} \quad (23)$$

where  $p$  is the external pressure. Only those for the stress  $\sigma_{rr}$  are not identically satisfied. The stress  $\sigma_{rr}$  on the boundaries is written in terms of the displacement field:

$$\sigma_{rr}(r_i, t) = c_{11} U_{,r}(r_i, t) + c_{12} \frac{U(r_i, t)}{r} + c_{13} f(t) - q_1 C(r_i, t), \quad i = 1, 2. \quad (24)$$

Substituting Eqs. (2), (8), (9) into (24) for  $U_0(r)$  gives the following two linear equations for  $G_{10}, G_{20}$ , and  $f_0$ :

$$\begin{aligned} (c_{11}\lambda_1 + c_{12})r_1^{\lambda_1-1}G_{10} + (c_{11}\lambda_2 + c_{12})r_1^{\lambda_2-1}G_{20} + A_0f_0 \\ = -c_{11}U_0^{*'}(r_1) - c_{12}\frac{U_0^*(r_1)}{r_1} + q_1[b_1 \ln(r_1/r_1) \\ + b_2 \ln(r_2/r_1)] + p_i \quad i = 1, 2, \end{aligned} \quad (25a)$$

where

$$A_0 = \frac{c_{11} + c_{12}}{c_{11} - c_{22}} (c_{23} - c_{13}) + c_{13} \quad \text{for } c_{11} \neq c_{22}$$

$$= \frac{c_{23} - c_{13}}{2c_{11}} [c_{11} + (c_{11} + c_{12}) \ln(r_1/r_1)] + c_{13} \quad \text{for } c_{11} = c_{22} \quad (25b)$$

and  $p_i = 0$ , at  $i = 1$ ;  $p_i = -p$  at  $i = 2$ .

In a similar fashion, by substituting the expressions for  $R_n(r)$ , there correspond two linear equations for  $G_{1n}, G_{2n}, f_n$ , for  $n = 1, \dots, \infty$ , as follows:

$$\begin{aligned} (c_{11}\lambda_1 + c_{12})r_i^{\lambda_1-1}G_{1n} + (c_{11}\lambda_2 + c_{12})r_i^{\lambda_2-1}G_{2n} + A_0f_n \\ = -c_{11}R_n^{*'}(r_i) - c_{12}\frac{R_n^*(r_i)}{r_i} + q_1[c_n J_0(r_i\alpha_n) + d_n Y_0(r_i\alpha_n)]; \end{aligned} \quad i = 1, 2. \quad (25c)$$

Now let us consider the conditions of resultant forces and moments. Since the stresses do not depend on  $z$ , these conditions exist in any cross-section. It can be proved (e.g., Lekhnitskii, 1963, although hygroscopic effects are not included) that the conditions of zero resultant forces along the  $x$  and  $y$ -axes of a Cartesian coordinate system are satisfied identically. The conditions of zero resultant moment along  $x$  and  $y$ -axes (and that of zero twisting moment) are also satisfied by the symmetry of the problem. Therefore, it remains only the condition of resultant axial force,  $P_z$ , arising in a hydrostatic field:

$$\int_{r_1}^{r_2} \sigma_{zz}(r, t) 2\pi r dr = P_z(t) = -p\pi(r_2^2 - r_1^2). \quad (26)$$

This gives the last set of equations that are needed to determine the constants  $G_{ij}, f_j$ . In terms of

$$q_3 = c_{13}\beta_r + c_{23}\beta_\theta + c_{33}\beta_z, \quad (27)$$

Eq. (26) gives

$$\begin{aligned} \left( \frac{c_{13}\lambda_1 + c_{23}}{\lambda_1 + 1} \right) (r_2^{\lambda_1+1} - r_1^{\lambda_1+1}) G_{10} + A_1 G_{20} + A_2 f_0 = (c_{13} - c_{23}) I_0 \\ + \frac{q_3}{2} \left[ \frac{(r_2^2 - r_1^2)}{2} (b_2 - b_1) + (r_2^2 b_1 - r_1^2 b_2) \ln(r_2/r_1) \right] \\ - \frac{p}{2} (r_2^2 - r_1^2) + c_{13} \sum_{i=1,2} (-1)^{i+1} r_i U_0^*(r_i), \end{aligned} \quad (28a)$$

and for  $n = 1, \dots, \infty$ ,

$$\begin{aligned} \left( \frac{c_{13}\lambda_1 + c_{23}}{\lambda_1 + 1} \right) (r_2^{\lambda_1+1} - r_1^{\lambda_1+1}) G_{1n} + A_1 G_{2n} + A_2 f_n \\ = (c_{13} - c_{23}) I_n + c_{13} \sum_{i=1,2} (-1)^{i+1} r_i R_n^*(r_i) \\ + (q_3/\alpha_n) (-1)^i [c_n r_i J_1(r_i\alpha_n) + d_n r_i Y_1(r_i\alpha_n)], \end{aligned} \quad (28b)$$

where  $I_0$  and  $I_n$  are given in Appendix C. The coefficients  $A_1, A_2$  are defined as

$$\begin{aligned} A_1 = \left( \frac{c_{13}\lambda_2 + c_{23}}{\lambda_2 + 1} \right) (r_2^{\lambda_2+1} - r_1^{\lambda_2+1}) \quad \text{for } c_{11} \neq c_{22} \\ = (c_{23} - c_{13}) \ln(r_2/r_1) \quad \text{for } c_{11} = c_{22} \end{aligned} \quad (29a)$$

$$\begin{aligned} A_2 = \frac{r_2^2 - r_1^2}{2} \left( c_{33} + \frac{c_{23}^2 - c_{13}^2}{c_{11} - c_{22}} \right) \quad \text{for } c_{11} \neq c_{22} \\ = \frac{(r_2^2 - r_1^2)}{8c_{11}} [4c_{33}c_{11} - (c_{23} - c_{13})^2] \\ + \frac{c_{23}^2 - c_{13}^2}{4c_{11}} r_2^2 \ln(r_2/r_1) \quad \text{for } c_{11} = c_{22}. \end{aligned} \quad (29b)$$

Therefore, the constants  $f_j, G_{ij}$  and hence the displacement  $U$

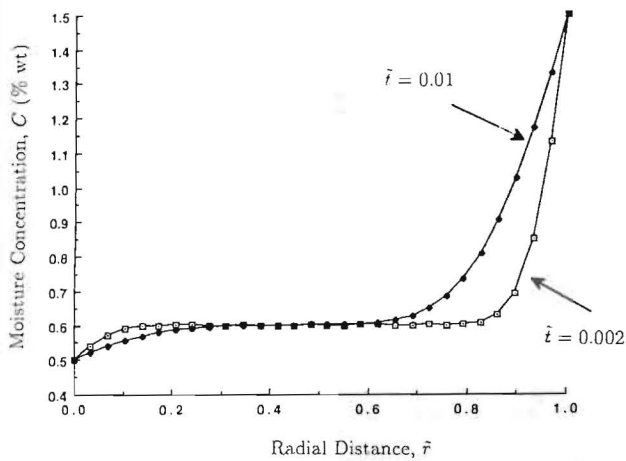


Fig. 2 Radial distribution of the concentration  $C(r, t)$  at different times. The nondimensional time is defined by  $\tilde{t} = Dt/(r_2 - r_1)^2$ . The nondimensional radial distance is defined by  $\tilde{r} = (r - r_1)/(r_2 - r_1)$ .

can be found by solving (25) and (28). After obtaining the displacement field, the stresses can be found by substituting in (6) and (3).

### Results and Discussion

First, a significant observation is that due to the slow rate of moisture diffusion, many terms, i.e., roots  $\alpha_n$  of the characteristic Eq. (2c), are needed, which makes the Hankel asymptotic regime very important. In the results presented in this section, 15 terms were used.

As an illustrative example, a T300/5208 Gr/Ep circular cylinder of inner radius  $r_1 = 20$  mm and radii ratio  $r_2/r_1 = 1.50$  was considered. The fibers are oriented along the circumferential direction. The typical values of moduli in  $\text{GN/m}^2$  and Poisson's ratios are as follows:  $E_1 = 9.9$ ,  $E_2 = 140$ ,  $E_3 = 9.1$ ,  $G_{23} = 4.3$ ,  $G_{12} = 4.7$ ,  $G_{31} = 5.9$ ,  $\nu_{12} = 0.020$ ,  $\nu_{23} = 0.30$ ,  $\nu_{31} = 0.49$ , where 1 is the radial ( $r$ ), 2 is the circumferential ( $\theta$ ), and 3 is the axial ( $z$ ) direction. The typical values of hygroscopic expansion coefficients (e.g., Hahn, 1976) are  $\beta_r = \beta_z = 6.67 \times 10^{-3}/\text{wt percent}$ ,  $\beta_\theta = 0$ . For this material, the moisture diffusivity in the radial direction is  $D = 2.145 \times 10^{-13} \text{ m}^2/\text{sec}$ . This value was obtained by substituting a temperature of  $50^\circ\text{C}$  to the equation for the temperature-dependent moisture diffusivity in Hahn (1976).

To illustrate the results, the nondimensional radial distance  $\tilde{r} = (r - r_1)/(r_2 - r_1)$ , and normalized time  $\tilde{t} = Dt/(r_2 - r_1)^2$  are used. The initial concentration (at  $t = 0$ ) is taken  $C_0 = 0.1$ , whereas the concentrations at the ends for  $t > 0$  are  $C_1 = 0.5$  and  $C_2 = 1.5$ .

Figure 2 shows the spatial distribution of the concentration. Two time values,  $\tilde{t} = 0.002$  (corresponding to about 10 days) and  $\tilde{t} = 0.01$  (corresponding to about 50 days), are used. The major stresses are the hoop,  $\sigma_{\theta\theta}$ , and the axial one  $\sigma_{zz}$ , and these are shown in Figs. 3 and 4. The boundary layer effect is more clearly shown in the axial stress. Notice that these plots illustrate the cases with no mechanical load present, i.e., these stresses are induced purely from the hygroscopic effects. Although a normalization of the stresses would be generally desirable in presenting the results, it is our opinion that for this particular hygroelastic problem, absolute values give a more clear description of the resulting effects. It should also be mentioned that longer time scales are used because the equilibrium process of moisture absorption or desorption takes much longer than that of temperature.

The coupling of mechanical loading and hygroscopic effects is illustrated in Figs. 5 and 6 which show the hoop stress,  $\sigma_{\theta\theta}$ , and the axial one,  $\sigma_{zz}$ , for (a) applied external pressure only

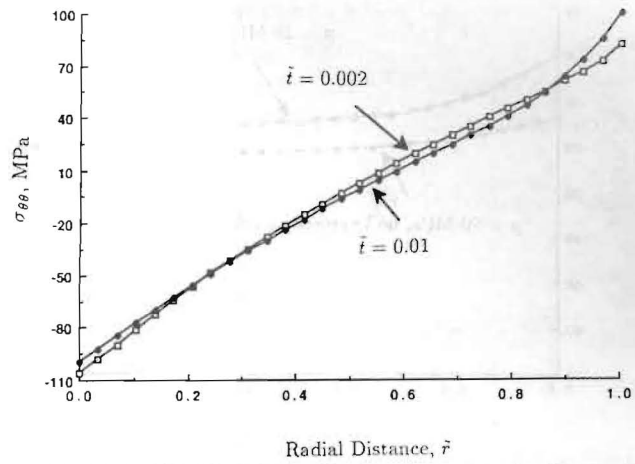


Fig. 3 Distribution of the hoop stress  $\sigma_{\theta\theta}$  (no mechanical loading)

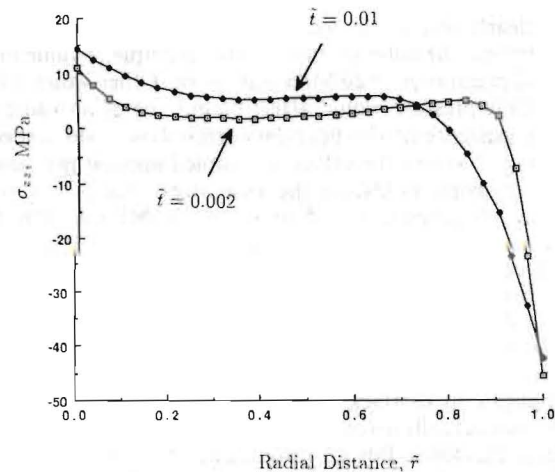


Fig. 4 Distribution of the axial stress  $\sigma_{zz}$  (no mechanical loading)

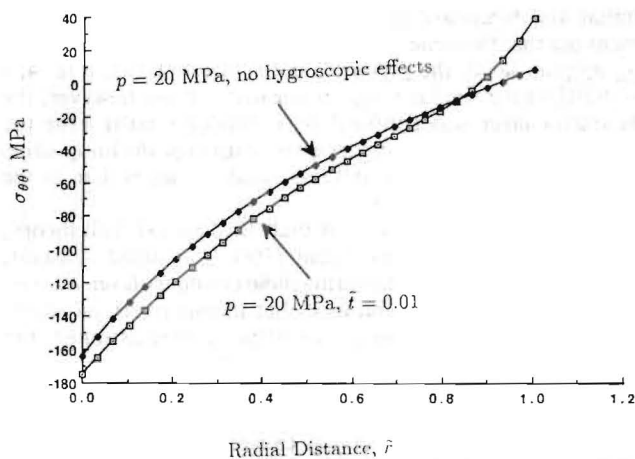


Fig. 5 Distribution of the hoop stress  $\sigma_{\theta\theta}$ , illustrating the coupling of mechanical loading (external pressure) and hygroscopic effects

and (b) applied external pressure with consideration of the hygroscopic effects at time  $\tilde{t} = 0.01$ . The stress distribution for hydrostatic pressure only is taken from Lekhnitskii (1981). It is seen that the hygroscopic effects result in an increase in the absolute value of the hoop stress at both the inner and outer boundaries. Again, the hygroscopic boundary layer is

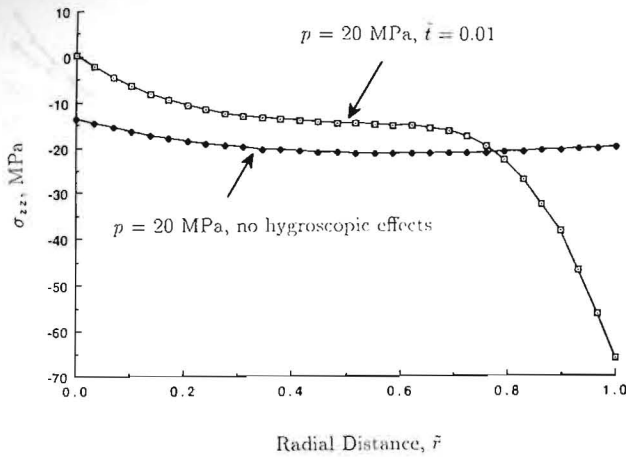


Fig. 6 Distribution of the axial stress  $\sigma_{zz}$  illustrating the coupling of mechanical loading (external pressure) and hygroscopic effects

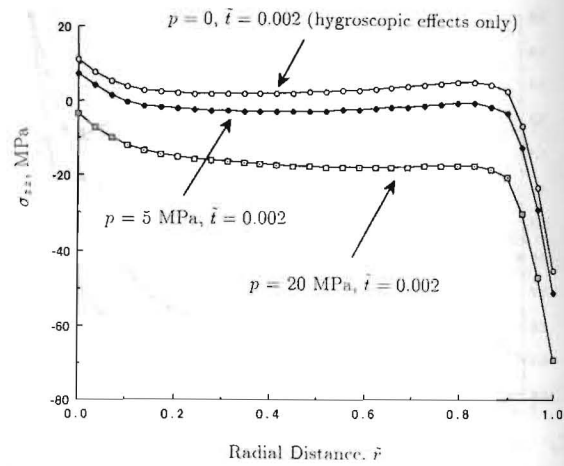


Fig. 7 Distribution of the axial stress  $\sigma_{zz}$  illustrating the effect of variable mechanical loading (external pressure) coupled with the hygroscopic effects

more clearly seen in the axial stress  $\sigma_{zz}$ , which shows a large increase near the outer surface. In this example, a value of the external pressure  $p = 20$  MPa was taken. Other values of the hydrostatic pressure would affect mainly the mean value and not the existence of the boundary stress layer. More specifically, Fig. 7 shows the effect of coupled applied pressure  $p$ , and hygroscopic fields, on the axial stress, for  $p = 0$  (only hygroscopic effects),  $p = 5$  and  $p = 20$  MPa at time  $\bar{t} = 0.002$ .

Notice also that for the example considered the reinforcement is along the periphery, thus the axial direction is a direction of weakness. Therefore, the boundary layer effect on the axial stress may have more important implications for failure initiation than a similar one on the hoop component.

Applications of thick composite shells in marine environments may actually involve a larger size than the one considered in these examples. For an insight into these size effects, the results for the transient stress profiles were derived for a shell made out of the same material with the same fiber orientation, and of inner radius  $r_1 = 4$  m and radii ratio  $r_2/r_1 = 1.25$ . A time value of 50 days with no mechanical loading and the same initial and boundary moisture concentrations were used. It turns out that the same boundary layer effect on the axial stress  $\sigma_{zz}$  appears (as in the present, smaller size example, Fig. 4,  $\bar{t} = 0.01$ ) with a similar range of negative values; however, the boundary layer was confined to a smaller  $\bar{r}$  range near the outer surface. A much smaller effect exists for the hoop stress  $\sigma_{\theta\theta}$ , with smaller positive and less negative values than in the small size example, Fig. 3.

A noteworthy observation is that the classical shell theory, in which the radial displacement  $U(r)$  is assumed constant, would not be capable of capturing these boundary layer stresses. Finally, it should be mentioned that in this paper moisture-independent material constants (stiffness) were assumed, but the moisture absorption may affect these constants as well. Moreover, the moisture diffusion process is accelerated or decelerated by temperature. In the future, it is desirable to consider these additional effects caused by coupled moisture and temperature fields. It is also desirable to examine the extent to which higher-order shell theories (e.g., Whitney and Sun, 1974; Librescu, 1975; Reddy and Liu, 1985) can predict this boundary layer stress field.

#### Acknowledgment

The financial support of the Office of Naval Research, Mechanics Division, Grant N00014-91-J-1892, and the interest and encouragement of the Project Monitor, Dr. Y. Rajapakse, are both gratefully acknowledged.

#### References

- Abramowitz, M., and Stegun, I. A., 1970, *Handbook of Mathematical Functions with Formulas, Graphs, and Mathematical Tables*, National Bureau of Standards Applied Mathematics Series No. 55, 9th Printing, Washington, D.C.
- Crank, J., 1975, *The Mathematics of Diffusion*, 2nd ed., Clarendon Press.
- Crossman, F. W., and Wang, A. S. D., 1978, "Stress Field Induced by Transient Moisture Sorptions in Finite-Width Composite Laminates," *Journal of Composite Materials*, Vol. 12, pp. 2-18.
- Doxee, L. E. Jr., and Springer, G. S., 1989, "Hygrothermal Stresses and Strains in Axisymmetric Composite Shells," *Computers and Structures*, Vol. 32, No. 2, pp. 395-407.
- Farley, G. L., and Herakovich, C. T., 1978, "Influence of Two Dimensional Hygrothermal Gradients on Interlaminar Stresses Near Free-Edges," *Advanced Composite Materials—Environmental Effects*, ASTM STP 658, J. Vinson, ed., ASTM, Philadelphia, PA, pp. 143-159.
- Hahn, H. T., 1976, "Residual Stresses in Polymer Matrix Composite Laminates," *J. Composite Materials*, Vol. 10, pp. 266-277.
- Kardomateas, G. A., 1989, "Transient Thermal Stresses in Cylindrically Orthotropic Composite Tubes," *ASME JOURNAL OF APPLIED MECHANICS*, Vol. 56, pp. 411-417; also Errata, *Ibid.*, 1991, Vol. 58, p. 909.
- Kardomateas, G. A., 1990, "The Initial Phase of Transient Thermal Stresses due to General Boundary Thermal Loads in Orthotropic Hollow Cylinders," *ASME JOURNAL OF APPLIED MECHANICS*, Vol. 57, pp. 719-724; also Errata, *Ibid.*, 1991, Vol. 58, p. 909.
- Lee, S. Y., and Yen, W. J., 1988, "Hygrothermal Effects on the Stability of a Cylindrical Composite Shell Panel," *ASME Aerospace Division AD*, Vol. 13, ASME, New York, pp. 21-31.
- Lekhnitskii, S. G., 1981, *Theory of Elasticity of an Anisotropy Body*, Mir Publishers, Moscow, pp. 124-128.
- Librescu, L., 1975, *Elastostatics and Kinetics of Anisotropic and Heterogeneous Shell-Type Structures*, Nordhoff International, Leyden.
- Reddy, J. N., and Liu, C. F., 1985, "A Higher-Order Shear Deformation Theory of Laminated Elastic Shells," *Int. J. Eng. Sci.*, Vol. 23, No. 3, pp. 319-330.
- Wang, S. S., and Choi, I., 1982, "Boundary-Layer Hygroscopic Stresses in Angle-Ply Composite Laminates," *AIAA Journal*, Vol. 20, No. 11, pp. 1592-1598.
- Whitney, J. M., and Husman, G. E., 1978, "Use of the Flexure Test for Determining Environmental Behavior of Fibrous Composites," *Experimental Mechanics*, Vol. 8, No. 5, pp. 185-190.
- Whitney, J. M., and Sun, C. T., 1974, "A Refined Theory for Laminated Anisotropic Cylindrical Shells," *ASME JOURNAL OF APPLIED MECHANICS*, Vol. 41, No. 2, pp. 471-476.
- Wylie, C. Ray, 1975, *Advanced Engineering Mathematics*, 4th ed., McGraw-Hill, New York.

#### APPENDIX A

The Bessel functions of first and second kind of order zero and one have a series expansion of the form (see, e.g., Wylie, 1975)

$$J_0(x) = \sum_{k=0}^{\infty} \frac{(-1)^k x^{2k}}{2^{2k} (k!)^2}; \quad J_1(x) = \sum_{k=0}^{\infty} \frac{(-1)^k x^{2k+1}}{2^{2k+1} k!(k+1)!} \quad (A1)$$

$$Y_0(x) = \frac{2}{\pi} \left( \ln \frac{x}{2} + \gamma \right) J_0(x) - \frac{2}{\pi} \sum_{k=1}^{\infty} \frac{(-1)^k x^{2k}}{2^{2k} (k!)^2} \psi(k), \quad (A2a)$$

$$Y_1(x) = \frac{2}{\pi} \left( \ln \frac{x}{2} + \gamma \right) J_1(x) - \frac{2}{\pi} \frac{1}{x} - \frac{1}{\pi} \sum_{k=0}^{\infty} \frac{(-1)^k x^{2k+1}}{2^{2k+1} (k!) (k+1)!} \left( 2\psi(k+1) - \frac{1}{k+1} \right). \quad (A2b)$$

In the above expressions  $\gamma = 0.577215 \dots$  is the Euler's constant and  $\psi(k)$  is defined as

$$\psi(k) = 1 + \frac{1}{2} + \dots + \frac{1}{k}. \quad (A2c)$$

The above series expansions can be used to calculate the Bessel's functions up to a value of the argument of about  $x = 18$ . They are rapidly convergent especially for small values of the argument.

Using the series expansion, we obtain the following equation in place of (10b):

$$c_{11} \left( R_n''(r) + \frac{R_n'(r)}{r} \right) - \frac{c_{22}}{r^2} R_n(r) = \frac{(c_{23} - c_{13}) f_n}{r} + \frac{c_n q_2 + (2/\pi)(q_1 + \gamma q_2) d_n}{r} + \frac{2d_n q_2 \ln(r\alpha_n/2)}{\pi r} + \frac{2d_n}{\pi} \sum_{k=0}^{\infty} \frac{(-1)^{k+1} \alpha_n^{2k+2} [q_2 + 2q_1(k+1)]}{2^{2k+2} [(k+1)!]^2} r^{2k+1} \ln(r\alpha_n/2) + \sum_{k=0}^{\infty} \frac{(-1)^{k+1} \alpha_n^{2k+2} f_{kn}}{2^{2k+2} [(k+1)!]^2} r^{2k+1}, \quad (A3)$$

where  $f_{kn}$  is defined in (13d).

For large arguments we can use the Hankel asymptotic expansions for the Bessel functions (see, e.g., Abramowitz and Stegun, 1970) to obtain the following expressions:

$$J_0(x) = A_0(x) \sin x + B_0(x) \cos x; \quad (A4a)$$

$$J_1(x) = B_1(x) \sin x - A_1(x) \cos x;$$

$$Y_0(x) = B_0(x) \sin x - A_0(x) \cos x;$$

$$Y_1(x) = -A_1(x) \sin x - B_1(x) \cos x. \quad (A4b)$$

The functions  $A_0(x)$ ,  $A_1(x)$ ,  $B_0(x)$ ,  $B_1(x)$  are given in terms of

$$\psi_1(k) = 1 \cdot 3 \cdot 5 \dots (4k-1)^2, \quad k=1, \infty; \quad \psi_1(0) = 1, \quad (A5)$$

as follows:

$$(\pi x)^{1/2} A_0(x) = \sum_{k=0}^{\infty} \frac{(-1)^k \psi_1(k)}{(2k)!(8x)^{2k}} \left[ 1 - \frac{16kx}{(4k-1)^2} \right], \quad (A6a)$$

$$(\pi x)^{1/2} A_1(x) = \sum_{k=0}^{\infty} \frac{(-1)^{k+1} \psi_1(k) (4k+1)}{(2k)!(8x)^{2k} (4k-1)} \times \left[ 1 - \frac{16kx}{(4k-3)(4k+1)} \right], \quad (A6b)$$

$$(\pi x)^{1/2} B_0(x) = \sum_{k=0}^{\infty} \frac{(-1)^k \psi_1(k)}{(2k)!(8x)^{2k}} \left[ 1 + \frac{16kx}{(4k-1)^2} \right], \quad (A6c)$$

$$(\pi x)^{1/2} B_1(x) = \sum_{k=0}^{\infty} \frac{(-1)^{k+1} \psi_1(k) (4k+1)}{(2k)!(8x)^{2k} (4k-1)} \times \left[ 1 + \frac{16kx}{(4k-3)(4k+1)} \right]. \quad (A6d)$$

In this way, the above series of the Hankel asymptotic expansion can be used to calculate the Bessel functions for values of the argument  $x \geq 18$ . The series converges rapidly and the number of terms required in the summation over  $k$  is at most 13 at  $x = 18.0$ , being smaller for larger values of the argument.

## APPENDIX B

In the event that for a certain  $k$ ,  $c_{11}(2k+3)^2 = c_{22}$ , the term in the sum in (13b) and (15b) for this  $k$  is

$$B_{1nk} r^{2k+3} \ln^2(r\alpha_n/2) + B_{2nk} r^{2k+3} \ln(r\alpha_n/2), \quad (B1)$$

where now

$$B_{1nk} = \frac{2d_n (-1)^{k+1} \alpha_n^{2k+2} [q_2 + 2q_1(k+1)]}{\pi 2^{2k+2} [(k+1)!]^2 4c_{11}(2k+3)}, \quad (B2a)$$

$$B_{2nk} = \frac{(-1)^{k+1} \alpha_n^{2k+2}}{2^{2k+2} [(k+1)!]^2 2c_{11}(2k+3)} \times \left\{ f_{kn} - \frac{2d_n [q_2 + 2q_1(k+1)]}{2\pi(2k+3)} \right\}. \quad (B2b)$$

## APPENDIX C

For  $c_{11} \neq c_{22}$ , the expression for  $I_0$  in (28a) is

$$I_0 = \frac{q_2(b_1 r_2^2 - b_2 r_1^2)}{2(c_{11} - c_{22})} \ln(r_2/r_1) + \left[ \frac{(2q_1 - q_2)}{4(c_{11} - c_{22})} - \frac{q_2 c_{11}}{(c_{11} - c_{22})^2} \right] (b_1 - b_2) (r_2^2 - r_1^2), \quad (C1)$$

and the expressions for  $I_n$ ,  $n = 1, \dots, \infty$ , in (28b), for the small arguments domain, are

$$I_n = \sum_{i=1,2} (-1)^i \frac{r_i^2}{2} \left( B_{0n} - \frac{d_n q_2}{\pi(c_{11} - c_{22})} \right) + (-1)^i \frac{d_n q_2}{\pi(c_{11} - c_{22})} r_i^2 \ln(r_i \alpha_n/2) + S_n, \quad (C2a)$$

$$S_n = \sum_{i=1}^2 \sum_{k=0}^{\infty} (-1)^i B_{1nk} \frac{r_i^{2k+4}}{2k+4} \ln(r_i \alpha_n/2) + (-1)^i \left( B_{2nk} - \frac{B_{1nk}}{2k+4} \right) \frac{r_i^{2k+4}}{2k+4}. \quad (C2b)$$

For  $c_{11} = c_{22}$ , the expression for  $I_0$  is

$$8I_0 c_{11} = q_2(b_1 r_2^2 + b_2 r_1^2) \ln^2(r_2/r_1) + (q_2 - q_1)(b_1 - b_2)(r_2^2 - r_1^2) + [(2q_1 - q_2)(b_1 - b_2)r_2^2 + q_2(b_2 r_1^2 - b_1 r_2^2)] \ln(r_2/r_1), \quad (C3a)$$

and the expressions for  $I_n$ ,  $n = 1, \dots, \infty$ , again in the small arguments domain, are

$$I_n = \sum_{i=1,2} (-1)^i \frac{d_n q_2}{\pi 4c_{11}} r_i^2 \ln^2(r_i \alpha_n/2) + (-1)^i \left( \frac{B_{0n}}{2} - \frac{d_n q_2}{\pi 4c_{11}} \right) r_i^2 \ln(r_i \alpha_n/2) + (-1)^{i+1} \left( \frac{B_{0n}}{2} - \frac{d_n q_2}{\pi 4c_{11}} \right) \frac{r_i^2}{2} + S_n. \quad (C3b)$$

For large arguments with  $\rho_i = r_i \alpha_n$ ,

$$\alpha_n I_n = \sum_{i=1,2} (-1)^i \sum_{k=0}^{\infty} \left( p_{k,1}^n + \frac{S_{k,2}^n}{2k+1/2} \right) I_{c,k}(\rho_i) + \left( S_{k,1}^n - \frac{p_{k,2}^n}{2k+1/2} \right) I_{s,k}(\rho_i) - \frac{p_{k,2}^n}{2k+1/2} \rho_i^{-2k-1/2} \cos \rho_i - \frac{S_{k,2}^n}{2k+1/2} \rho_i^{-2k-1/2} \sin \rho_i, \quad (C4)$$

where  $I_{c,k}(\rho)$  and  $I_{s,k}(\rho)$  are defined by the recursive formulas

$$(2k-1/2)(2k-3/2)I_{c,k} = -(2k-3/2)\rho^{-2k+1/2} \cos \rho + \rho^{-2k+3/2} \sin \rho - I_{c,k-1}, \quad (C5a)$$

$$(2k-1/2)(2k-3/2)I_{s,k} = -(2k-3/2)\rho^{-2k+1/2} \sin \rho - \rho^{-2k+3/2} \cos \rho - I_{s,k-1}. \quad (C5b)$$

The process starts from  $k = 0$ , and initially,

$$I_{c,0}(\rho) = \int \rho^{-1/2} \cos \rho d\rho; \quad I_{s,0}(\rho) = \int \rho^{-1/2} \sin \rho d\rho. \quad (C5c)$$

Notice that the integral of the homogeneous solution (22a) (due to continuity requirements at the transition point of the two partial solutions) should be added to  $I_n$ , i.e., for  $c_{11} \neq c_{22}$ , the following term should be added:

$$\sum_{i=1,2} (-1)^i \left( h_1 \frac{\rho_i^{\lambda_1+1}}{\lambda_1+1} + h_2 \frac{\rho_i^{\lambda_2+1}}{\lambda_2+1} \right). \quad (C6)$$

For  $c_{11} = c_{22}$ , the term multiplying  $h_2$  in the previous relation (C6) is  $\ln \rho_i$ .

(continued from page 130)

### C—Experimental Studies, Operating Experiences, and Failure Analysis

- 1 Residual life prediction, life-time extension, availability
- 2 Small and large-scale experimental techniques
- 3 Scale-up approaches
- 4 Preventive maintenance and repair schedules
- 5 Feed-back from failure analysis

### D—Codes and Standards, Quality Assurance, Nondestructive Testing and Inspection

- 1 Quality assurance from design to start-up
- 2 Non-destructive examination techniques
- 3 Inspection strategies, surveillance and operational monitoring
- 4 Repair procedures and assessment of integrity

A panel discussion on international developments in standards, rules and codes will be organized independently on the base of invited papers from panel members.

Authors wishing to offer a paper for presentation at the conference must forward three copies of an abstract to the Regional Committee relevant to their geographical area (see below), indicating to which group of topics the paper belongs. Abstracts should be approximately 200 words, and should highlight new findings to be discussed in the paper. The name, complete mailing address, and FAX number of all authors must be submitted. In the case of several contributors to an abstract, a corresponding author should be designated.

**The European-African Regional Committee** (Europe, Africa and Russia) to Mr. Peter J. Willows, Institution of Mechanical Engineers (IMechE), 1 Birdcage Walk, London SW1H, U.K.; Fax: (44)-071-233-1654.

**The Americas Regional Committee** (Canada, U.S.A. and all countries in South America and Central America) to Prof. G.E.O. Widera, Mechanical and Industrial Engineering Department, Marquette University, 1515 W. Wisconsin Avenue, Milwaukee, WI 53233; Fax: (1)-414-288-1647.

**The Asian and Oceanic Regional Committee** (Countries in Asia and in the Pacific and Indian Oceans including Australia and New Zealand) to Prof. I. Iida, Department of Mechanical Engineering, Shibaura Institute of Technology; 3-9-14, Shibaura, Minato-ku, Tokyo, Japan; Fax: (81)-489-78-7796.

Abstracts will be accepted until *31 August 1994*.

Authors will be advised of the status of their abstract by *31 December 1994*.

Authors selected will be invited to prepare a draft of their complete paper, which must be sent to the appropriate Regional Committee by *30 April 1995*.

Drafts will be reviewed and authors informed by *30 June 1995*, of the status of their paper, and whether any modifications are required.

Authors will be invited to prepare the final manuscript and will receive instructions and guidance on the format, including figures and diagrams. The final manuscript is required by *30 November 1995*.